Electronic Supplementary Material (ESI) for Nanoscale Horizons.

Supplemental Information:

Role of Carboxylates in the Phase Determination of Metal Sulfide Nanoparticles

Andrey A. Shults,[a,b] Guanyu Lu,[b,c] Joshua D. Caldwell,[a,b,c] and Janet E. Macdonald,[a,b]*

[a]Department of Chemistry, Vanderbilt University, Nashville TN 37235, USA

[b]Vanderbilt Institute for Nanoscale Science and Engineering, Nashville TN 37235, USA

[c]Department of Mechanical Engineering, Vanderbilt University, Nashville TN 37235, USA.

Contents

1. Nuclear Magnetic Resonance (NMR) Spectra

1.1 Full ^{1}H NMR Copper Temperature and Time Studies

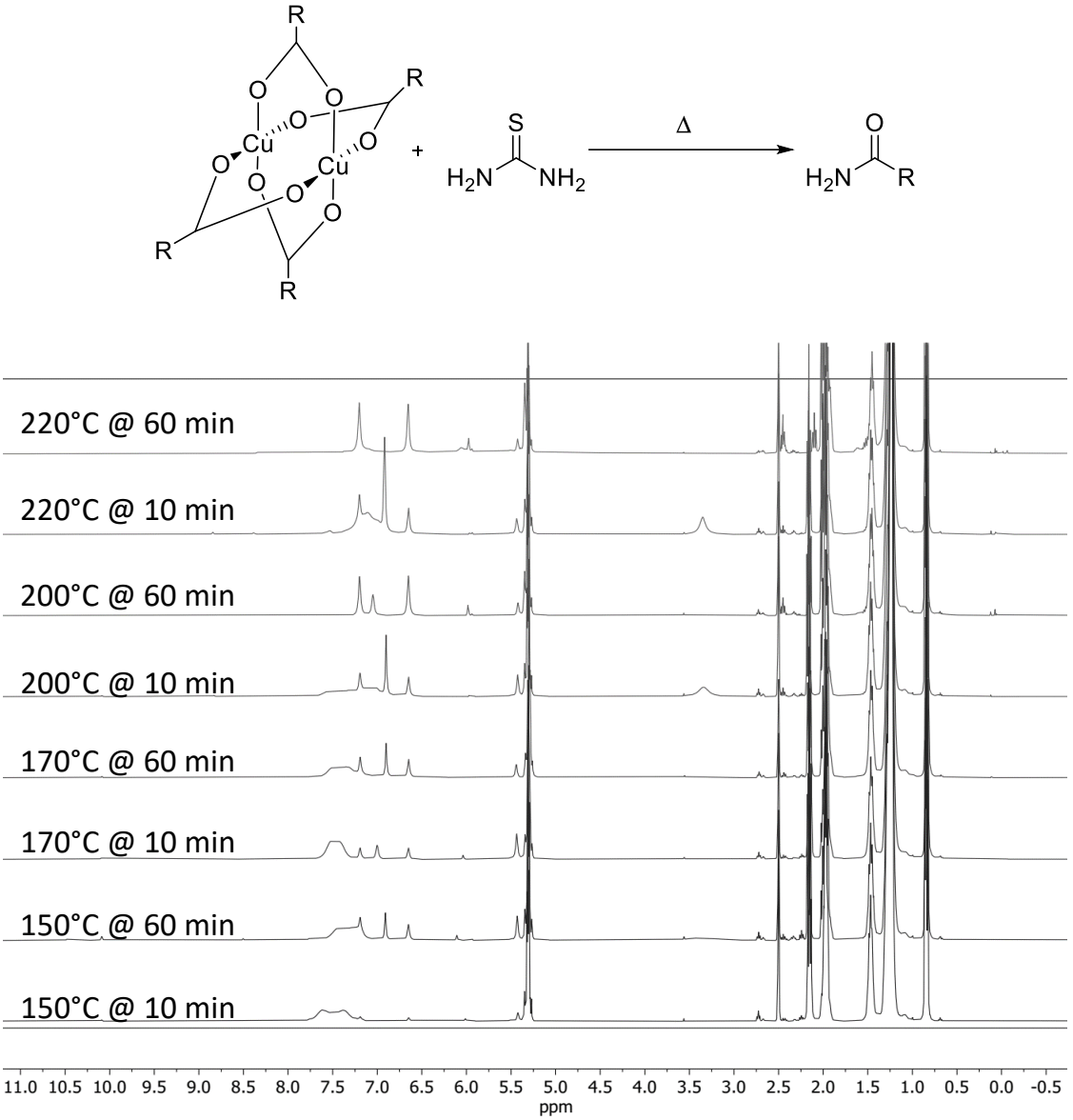

Figure S1. ^{1}H NMR temperature and time studies of the reaction between copper oleate and thiourea (neat). Formation of oleamide is detected starting at 150°C at ten minutes. NMR was run in DMSO-d_6.

Discussion of ^{1}H NMR Decomposition Studies (Metal Present)

Studies show the presence of oleate precursor in the upfield region. Increasing temperature and time decreases the relative integration of the beta hydrogen of oleic acid (2.15 ppm). Double bond signal (singlet) at 5.30 ppm remains unchanged with respect to temperature and time. Additionally, we see the formation of oleamide as evident from two singlets (6.66 and 7.21 ppm) responsible for the hydrogens of the amid group. Ammonium thiocyanate (7.00 – 7.21 ppm) byproduct can also be detected. See main document for further discussion.

1.2 Full ^{13}C NMR Copper Temperature and Time Studies

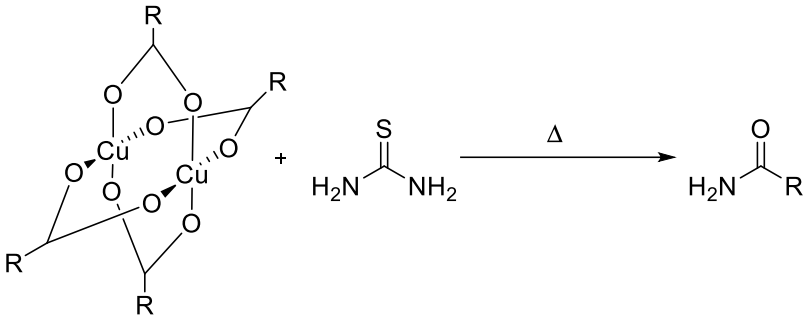

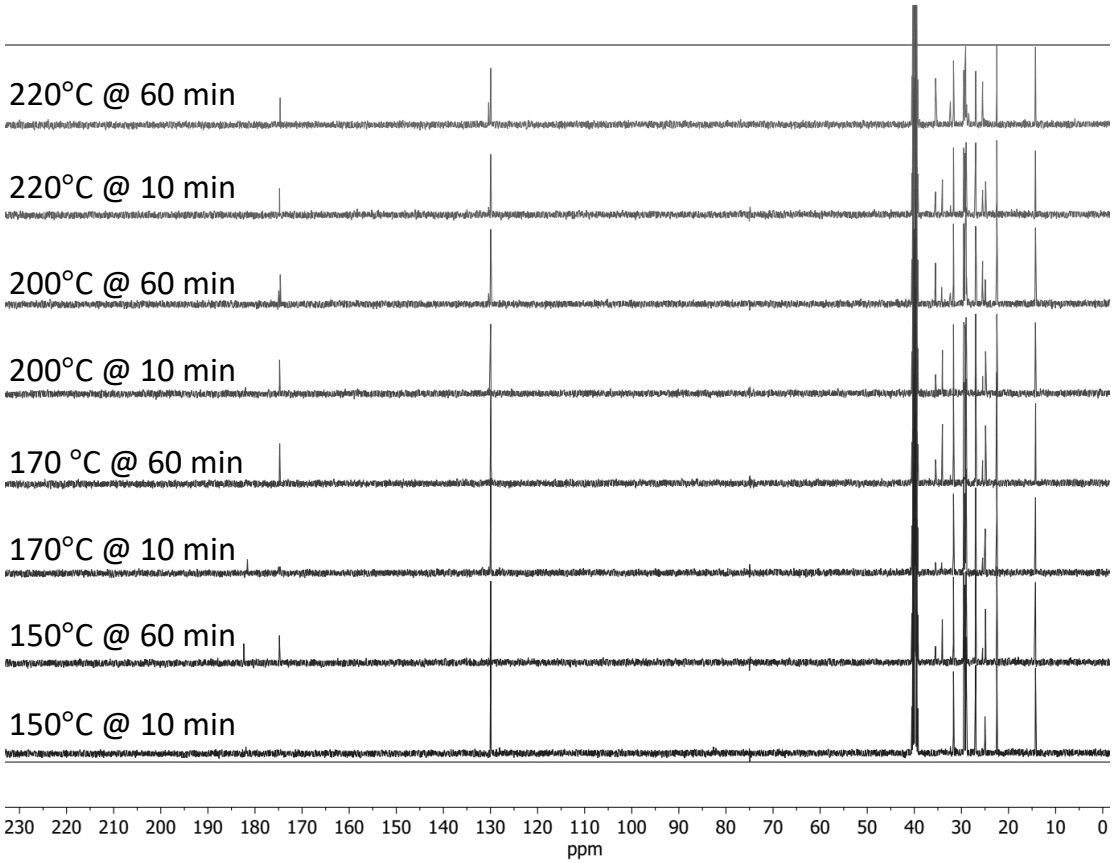

Figure S2. ^{13}C NMR temperature and time studies of the reaction between copper oleate and thiourea (neat). NMR was run in DMSO-d_6.

Discussion of ^{13}C NMR Decomposition Studies (Metal Present)

Studies show the presence of oleate precursor in the upfield region. Increasing temperature and time decreases the relative intensity of the beta carbon of oleic acid (34 ppm). A signal at 36 ppm appears indicating transformation of oleic acid to oleamide.

1.3 Full ^{1}H NMR Non-Metal Temperature and Time Studies

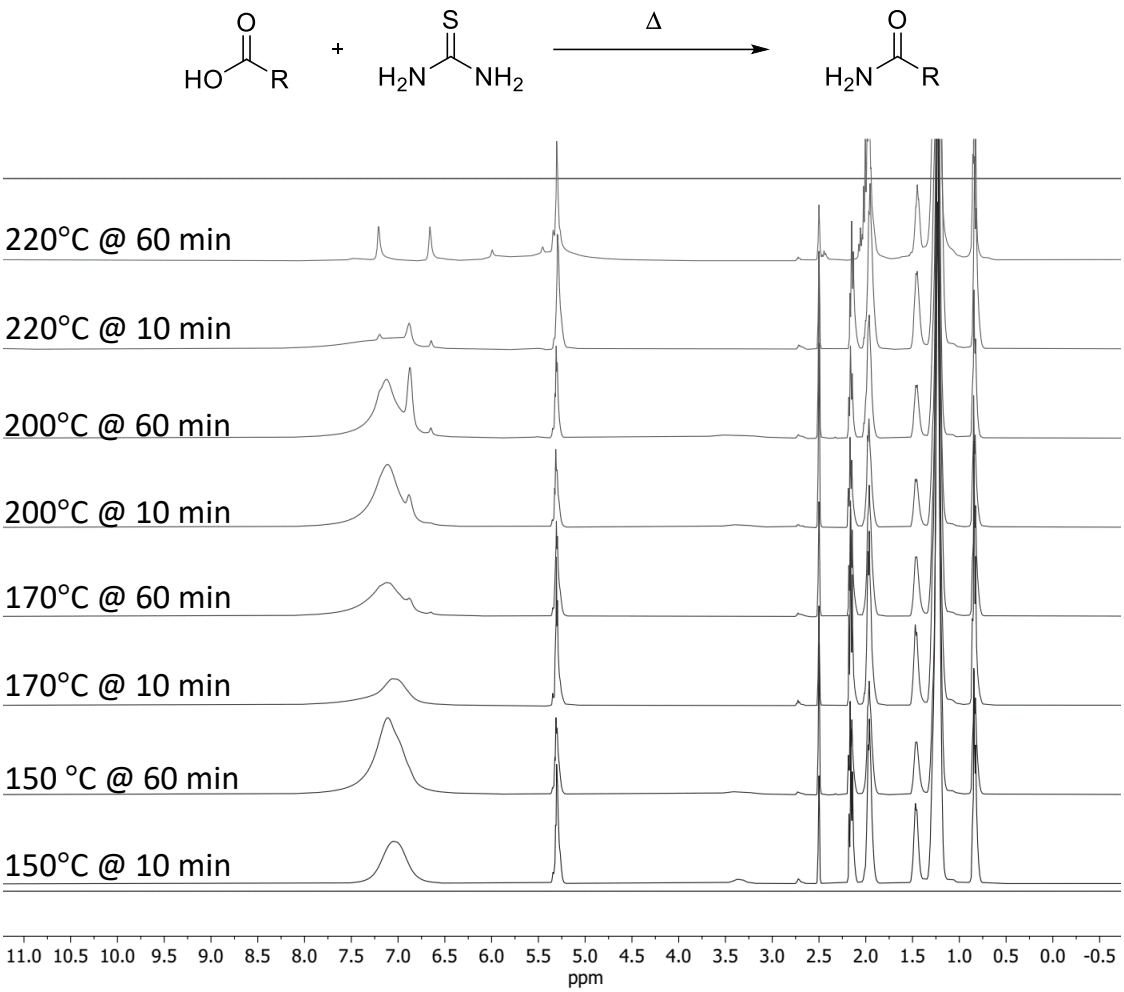

Figure S3. ^{1}H NMR temperature and time studies of the reaction between oleic acid and thiourea (neat). NMR was run in DMSO-d_6.

Discussion of ^{1}H NMR Decomposition Studies (Metal Absent)

NMR studies show that in the absence of the metal, oleamide does not form until 170°C at one hour. With the metal present, oleamide is seen formation at 150°C and ten minutes. This supports our claim that the metal is only promoting our reaction.

1.4 Full ^{1}H NMR Metal: Carboxylate Ratio Studies at Short Reaction Times

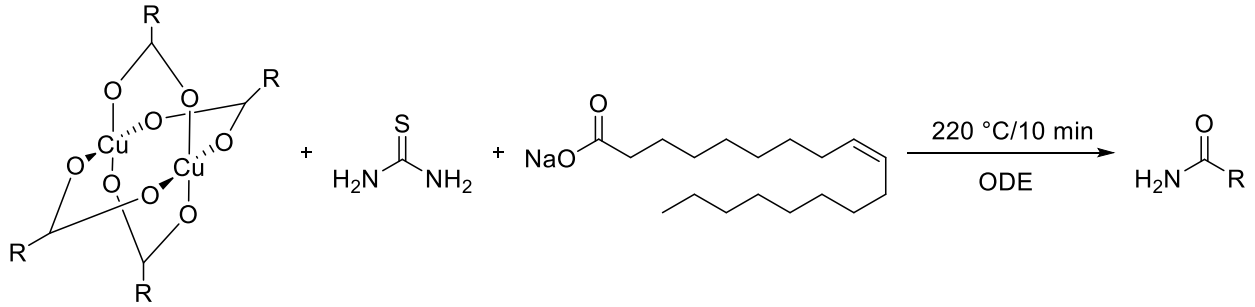

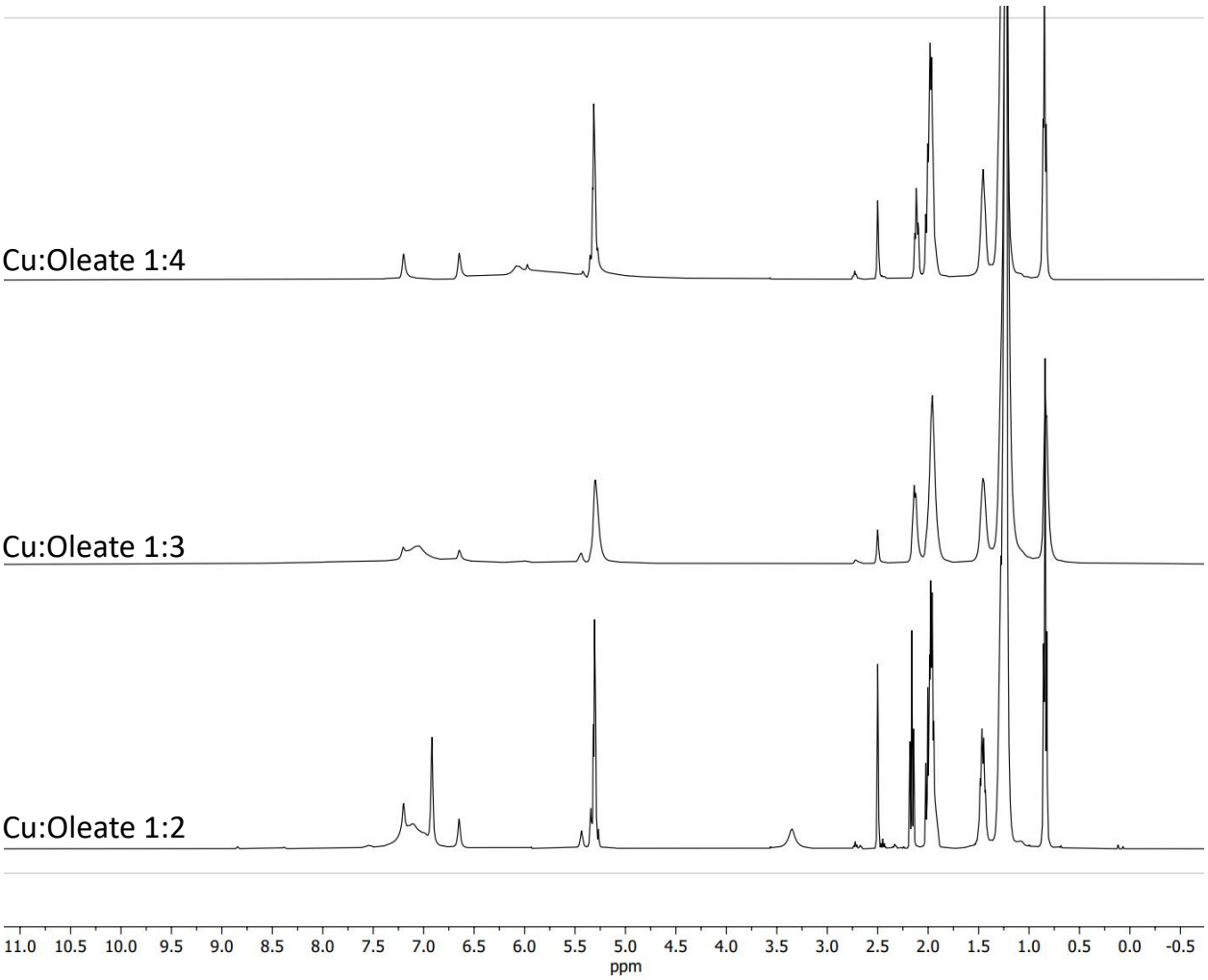

Figure S4. ^{1}H NMR of metal:carboxylate ratio studies for the ten minute reaction between copper oleate, sodium oleate, and thiourea (neat). NMR was run in DMSO-d_6.

1.5 Full ^{1}H NMR Metal: Carboxylate Ratio Studies at Long Reaction Times

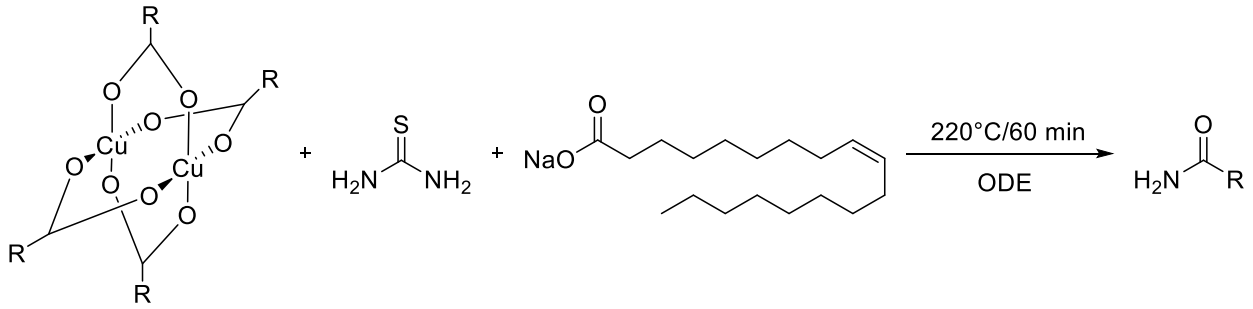

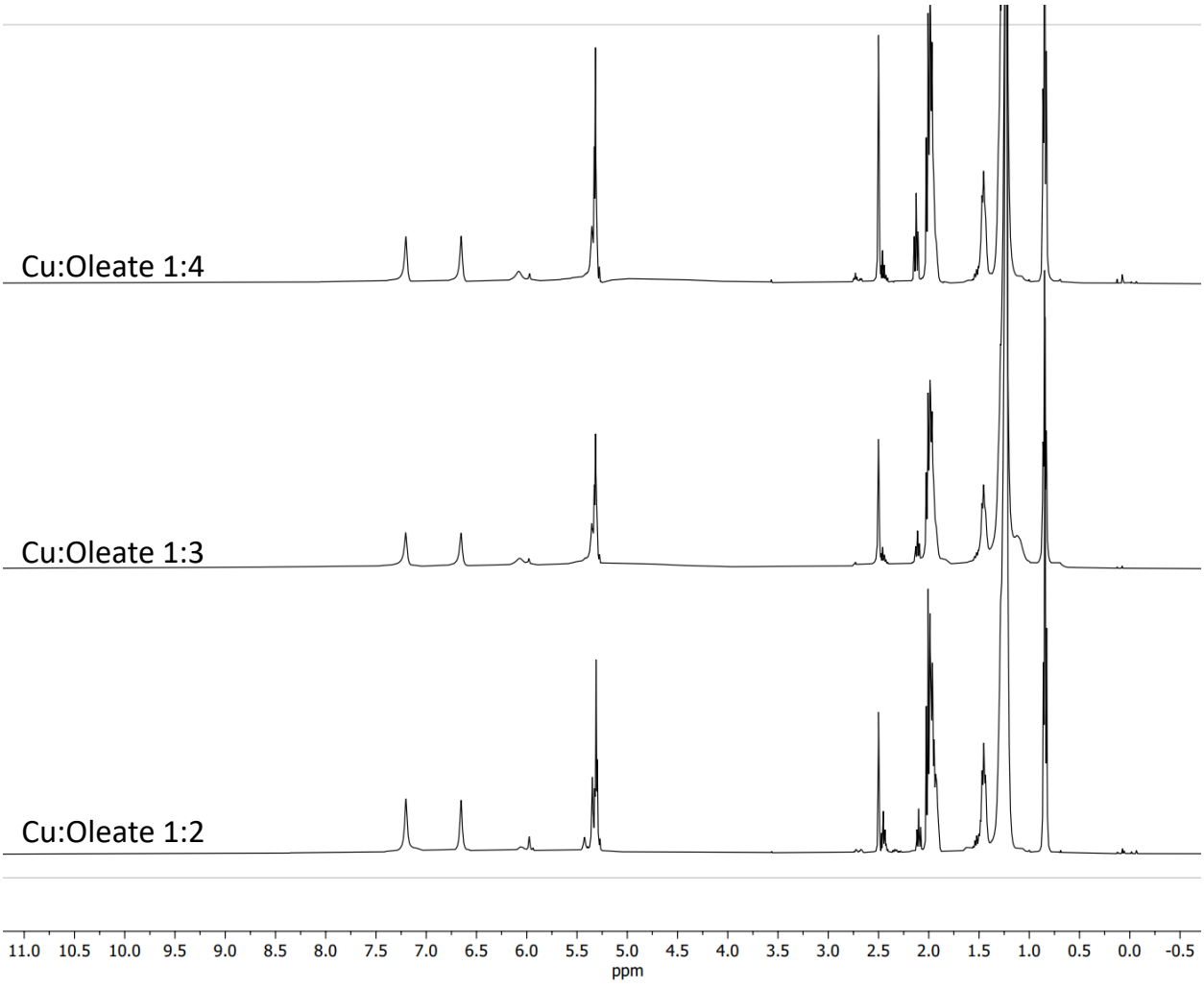

Figure S5. ^{1}H NMR of metal:carboxylate ratio studies for the 60 minute reaction between copper oleate, sodium oleate, and thiourea (neat). NMR was run in DMSO-d_6.

1.6 Full ^{1}H NMR Nickel Temperature and Time Studies

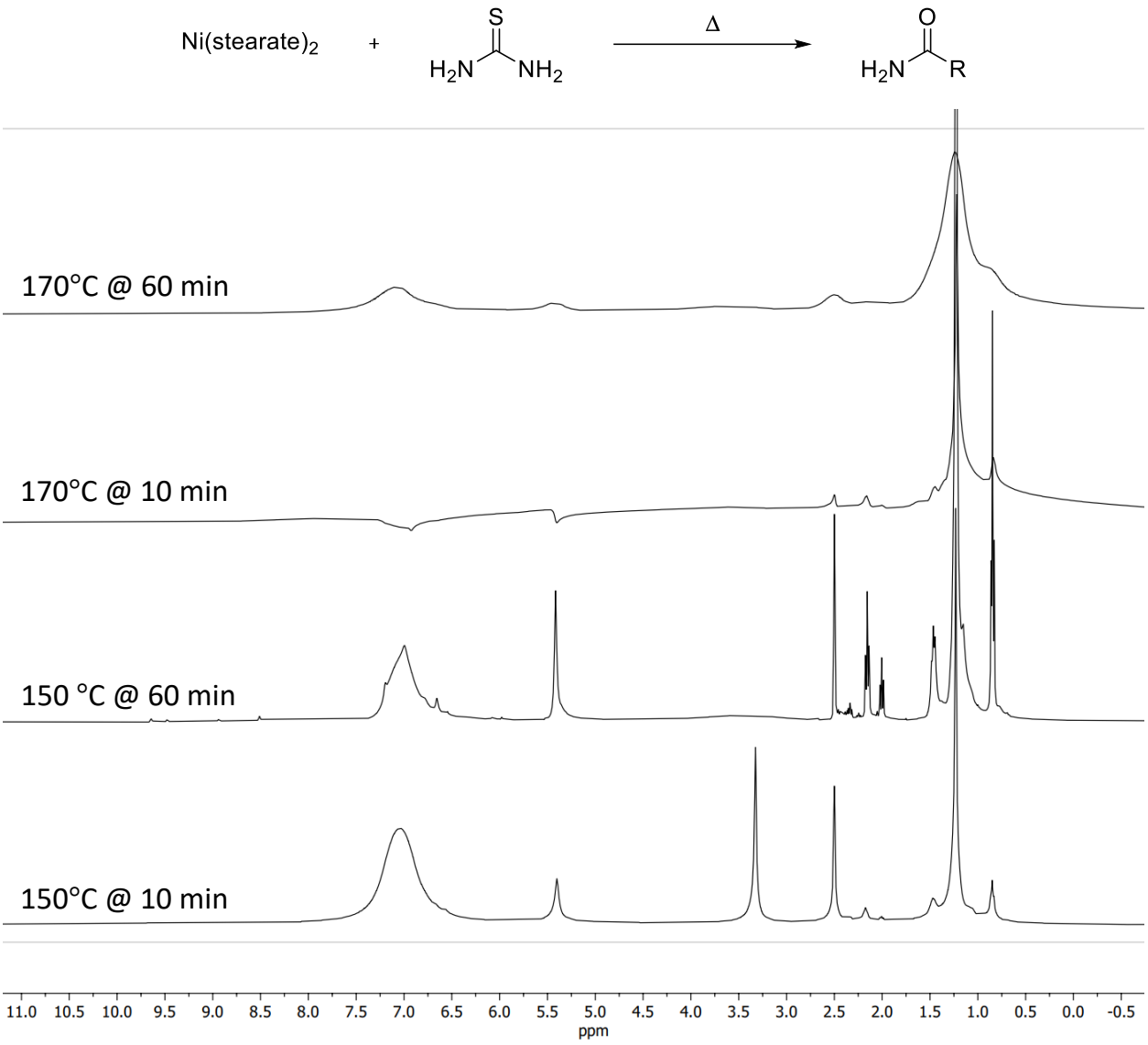

Figure S6. ^{1}H NMR temperature and time studies of the reaction between nickel stearate and thiourea (neat). NMR was run in DMSO-d_6.

1.7 Standards

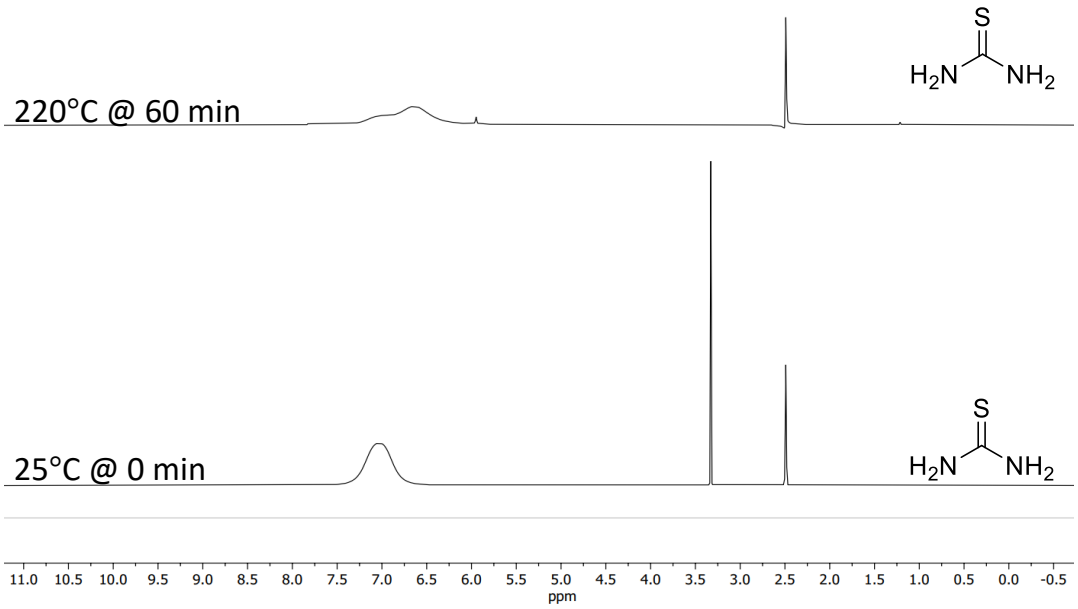

Figure S7. ^{1}H NMR of thermal decomposition of thiourea at 220°C for one hour (neat). NMR shows formation of melamine at 6.0 ppm. NMR was run in DMSO-d_6.

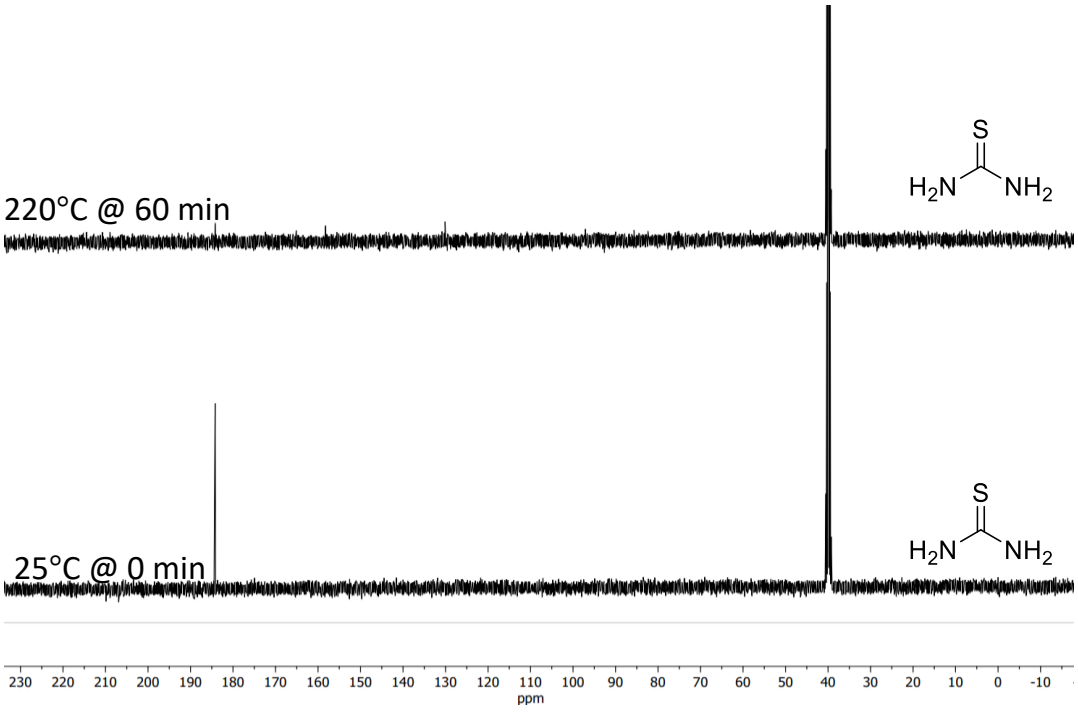

Figure S8. ^{13}C NMR of thermal decomposition of thiourea at 220°C for one hour (neat). NMR shows formation ammonium thiocyanate at 130 ppm.[1] NMR was run in DMSO-d_6.

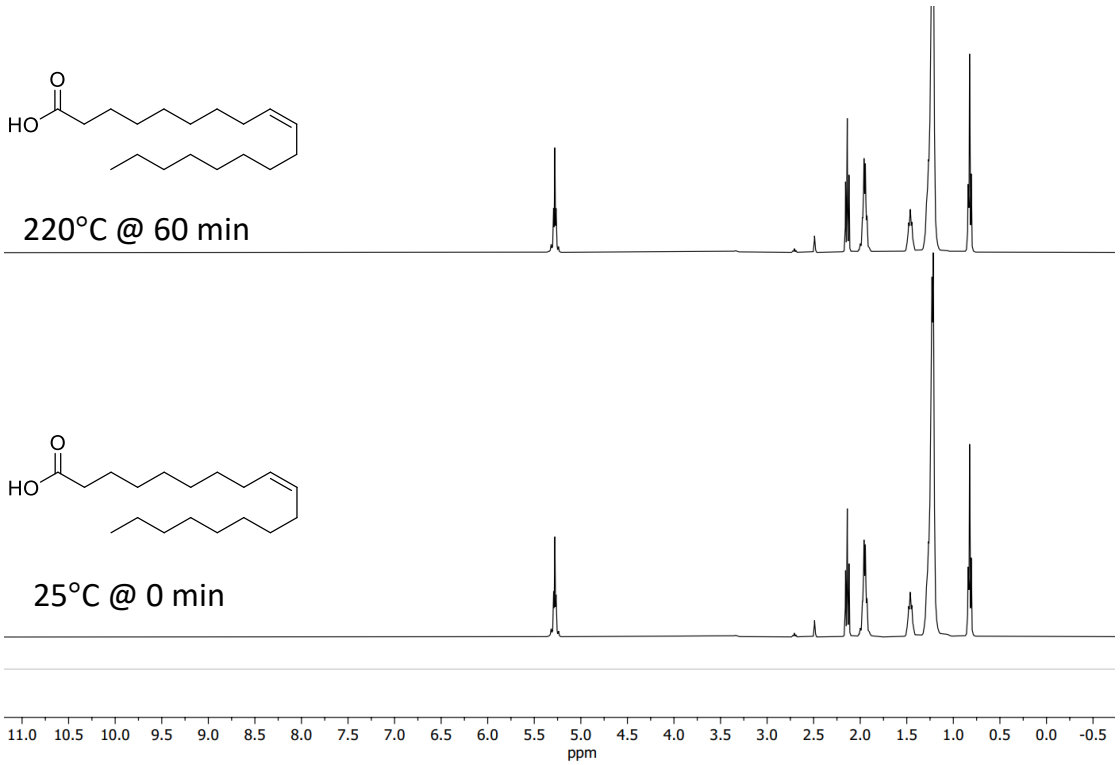

Figure S9. ^{1}H NMR of thermal decomposition of oleic acid at 220°C for one hour (neat). No decomposition was seen. NMR was run in DMSO-d_6.

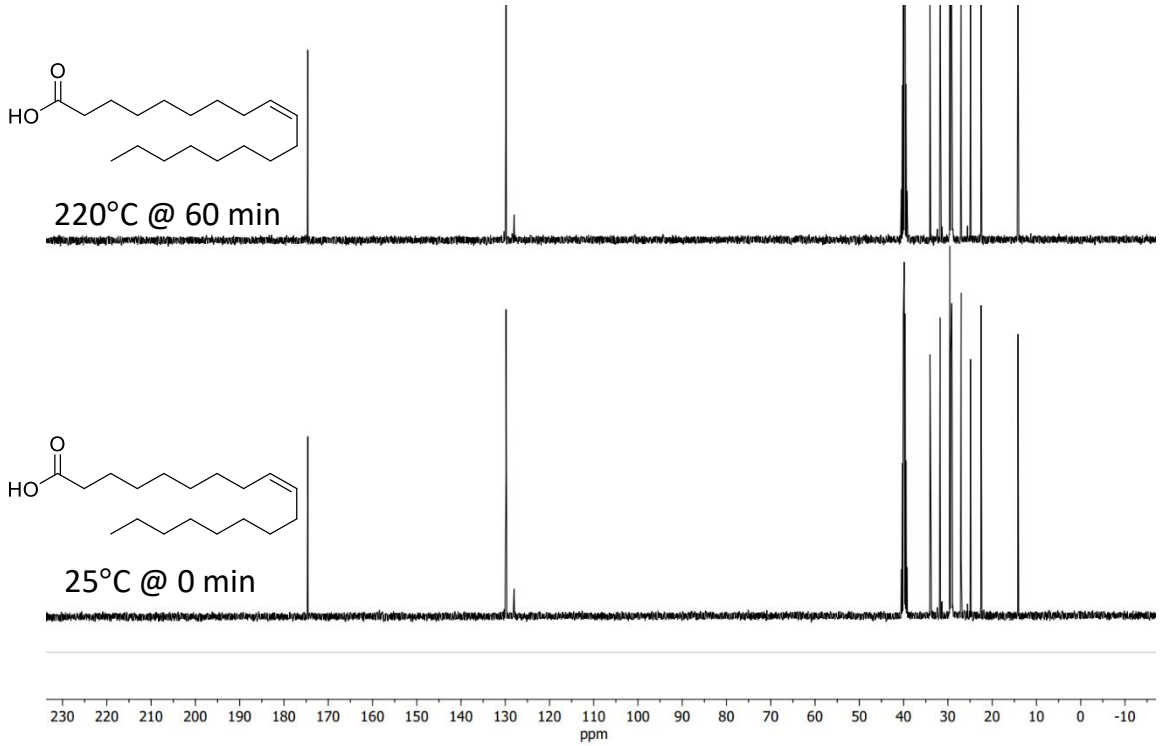

Figure S10. ^{13}C NMR of thermal decomposition of oleic acid in DMSO-d_6 at 220°C for one hour (neat). No decomposition was seen. NMR was run in DMSO-d_6.

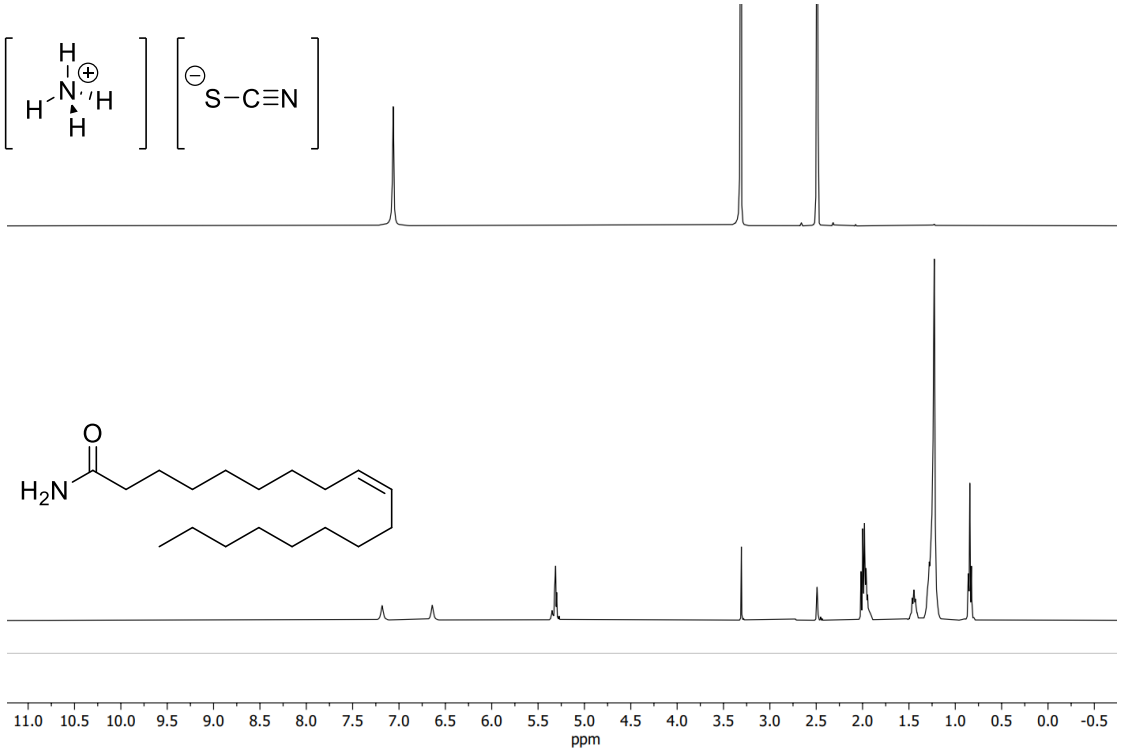

Figure S11. ^{1}H NMR of standards for oleamide (bottom) and ammonium thiocyanate (top) at room temperature (neat). NMR was run in DMSO-d_6.

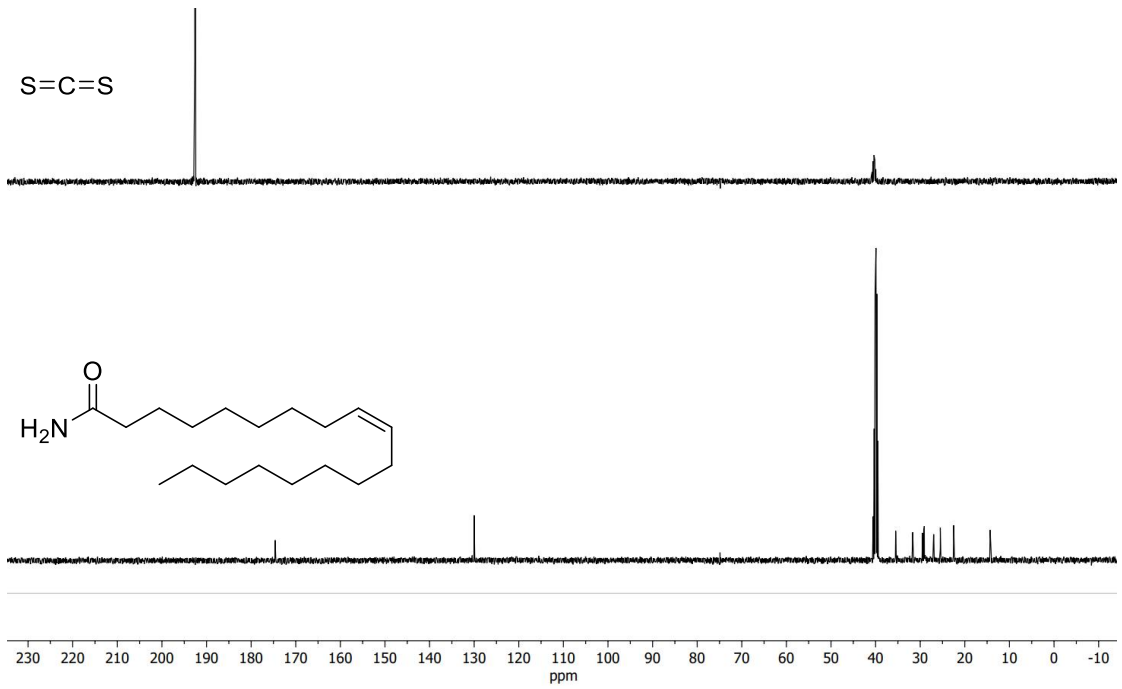

Figure S12. ^{13}C NMR of standards for oleamide (bottom) and carbon disulfide (top) at room temperature (neat). NMR was run in DMSO-d_6.

2. Powder X-ray Diffraction (pXRD) Pattern

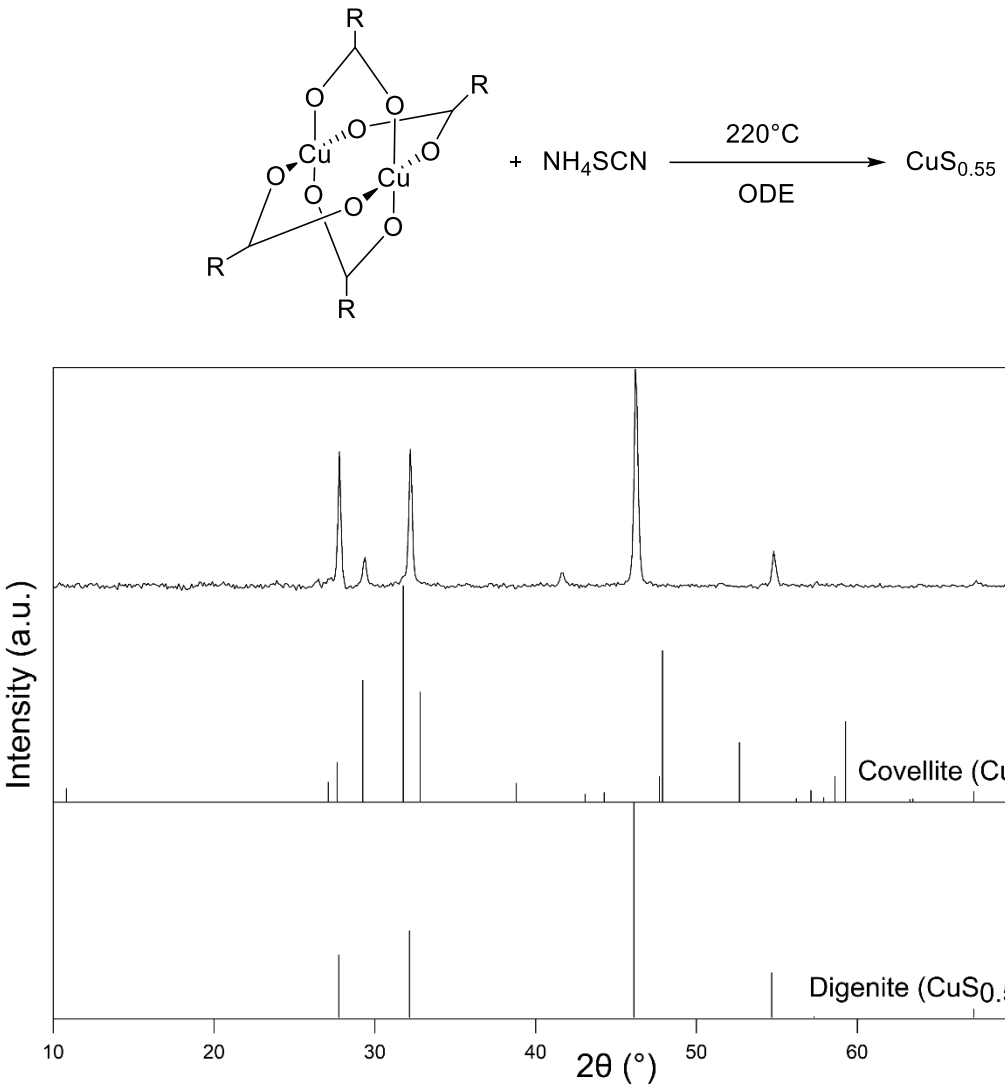

Figure S13. Powder X-Ray diffraction pattern of digenite ($CuS_{0.55}$) nanoparticles synthesized from copper oleate (0.5 mmol) and ammonium thiocyanate (3.0 mmol) in ODE.

3. Gas Fourier Transform Infrared (FTIR) Spectra

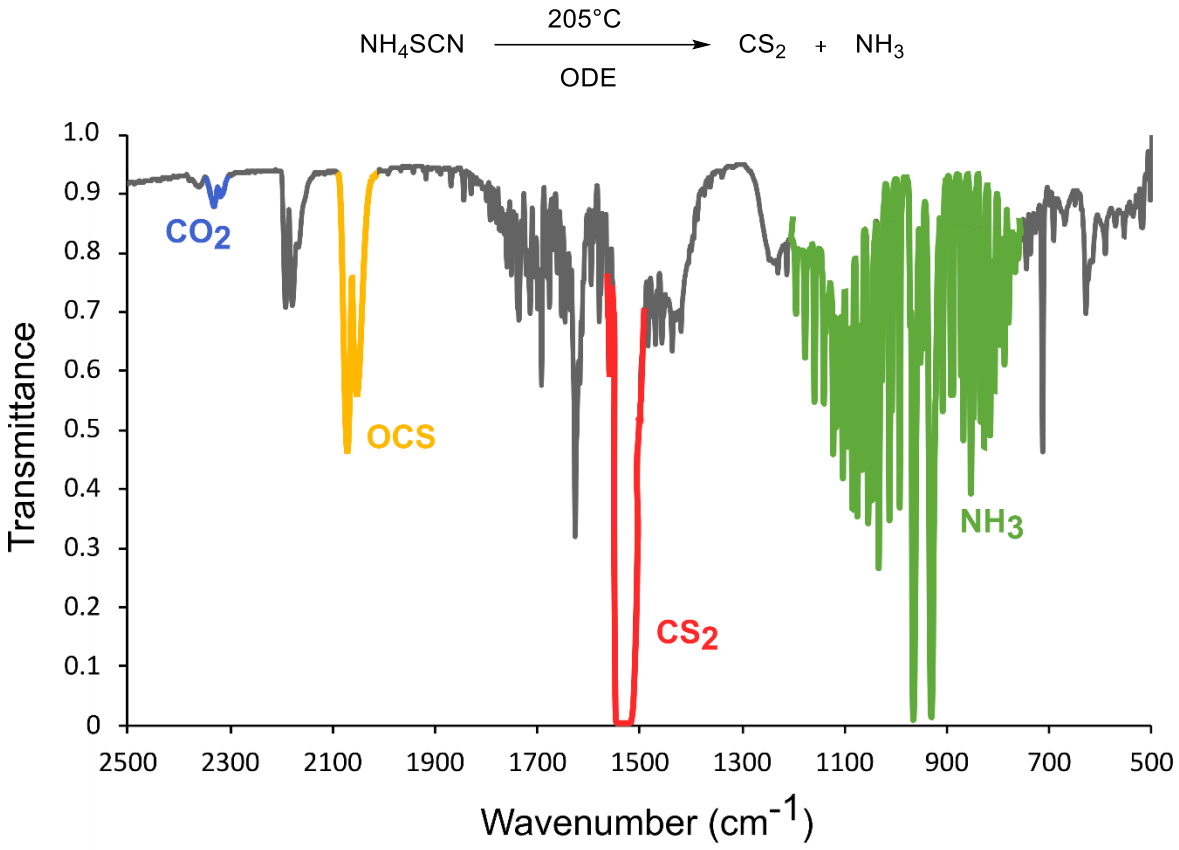

Figure S14. Gas FTIR of thermal decomposition products of ammonium thiocyanate (13 mmol) in ODE at 205°C. The following gases were observed: CO_2 (air contamination), OCS (air contamination), CS_2, and NH_3.

4. Attenuated Total Reflectance Fourier Transform Infrared (ATR-FTIR) Spectroscopy Standards

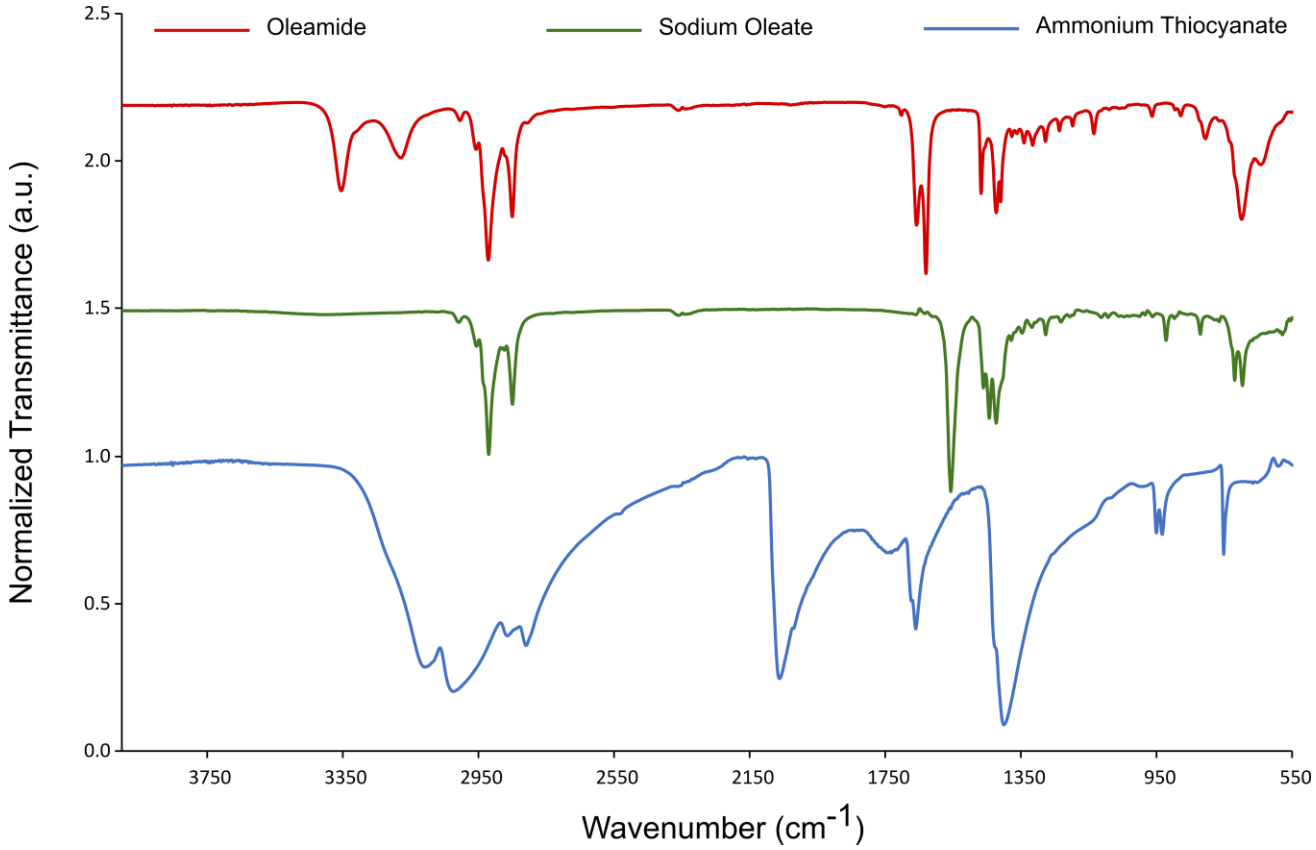

Figure S15. ATR-FTIR spectra of precursor and decomposition by-product standards including oleamide (top, red), sodium oleate (middle, green), ammonium thiocyanate (bottom, blue) taken at room temperature.

5. Metal Sulfides: Thermodynamics and Phase Trends

5.1 Experimental Trends

Table S1. Nanoparticle trends with respect to sodium oleate concentration

Metal	Cu	Ni	Fe	Co
Phase at Low [Carboxylate]	Covellite (CuS)	Vaesite (NiS_2)	Marcasite (FeS_2), Pyrite (FeS_2), Smythite ($FeS_{1.3}$), Greigite ($FeS_{1.3}$)	Catterite (CoS_2)
Phase at High [Carboxylate]	Digenite ($CuS_{0.56}$)	Nickel Sulfide (NiS)	Pyrrhotite ($FeS_{1.1}$)	Jaipurite (CoS)
Sulfur Content Trend	Sulfur Decreased	Sulfur Decreased	Sulfur Decreased	Sulfur Decreased
Anion Packing Trend	Hexagonal to Cubic	Cubic to Hexagonal	Cubic and Hexagonal to Hexagonal	Cubic to Hexagonal

5.2 Phase Thermodynamics

Table S2. Enthalpies of Formation of Relevant Metal Sulfide Phases

Metal Sulfide Family	Phase	Chemical Formula	ΔH_f (kJ/mol)	Reference Author
Iron	Marcasite	FeS_2	-171.1	Grønvold[2]
	Pyrite	FeS_2	-169.5	Grønvold[2]
	Smythite	$FeS_{1.3}$	-150.0	Erd[3]
	Greigite	$FeS_{1.3}$	-144.1	Subramani[4]
Copper	Digenite	$CuS_{0.55}$	-74.9	Waldner[5]
	Chalcocite	$CuS_{0.50}$	-81.6	Waldner[6]
	Djurleite	$CuS_{0.51}$	-81.8	Waldner[6]
Nickel	Nickel Sulfide	NiS	-88.1	Cemič[7]
	Millerite	NiS	-91.0	Cemič[7]
Cobalt	Cobalt Pentlandite	Co_9S_8	-885.7	Cemič[8]
	Jaipurite	CoS	-88.2	Rosenqvist[9]

6. Additional Methods

6.1 Synthesis of Copper Sulfide with Ammonium Thiocyanate

A solution of copper oleate (0.50 mmol) in octadecene (ODE) (10 mL) was added to a 25 mL three neck round-bottom flask. Ammonium thiocyanate (3.0 mmol) and ODE (5 mL) was added to an addition funnel, connected to round-bottom flask. The apparatus was placed under vacuum while the three-neck flask was heated to 100°C for 30 min. The flask was then heated to 220°C. The addition funnel was warmed with a heat gun to approximately 170°C (~5 min), to allow the ammonium thiocyanate to dissolve in the ODE, and then the contents added swiftly to the round-bottom flask. The solution was continuously stirred at 1100 rpm and kept in the reaction vessel for 60 min. Nanoparticle products were isolated by precipitation with ethanol (10-25 mL), centrifugation, and resuspension with chloroform (3-10 mL) three times. The higher volumes of washing solvents were used with high-oleate reactions.

6.2 NMR Calculation of Oleamide to Oleate Ratio

To monitor the rate of the side reaction with respect to the sodium oleate, the relative concentrations of the amide and thiourea can be compared. The hydrogens of oleamide that are positioned on carbon number two overlap with the hydrogens positioned on carbons next to the double bond **(Figure 2B,C)**. In contrast, the hydrogens on carbon two of sodium oleate can be distinguished from the hydrogens next to its double bond **(Figure 2A,C)**. These two hydrogens on sodium oleate can be compared (using integrations) to the two hydrogens of the amide group to plot the relationship between the two molecules **(Figure 2D)**.

6.3 Glassware Set-Up for Metal Sulfide Synthesis

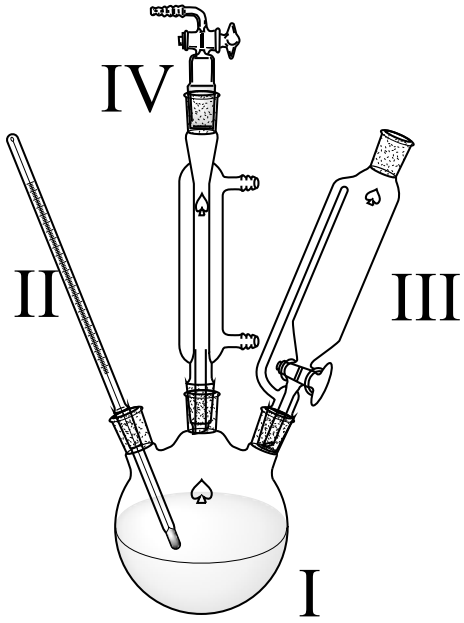

Figure S16. Experimental set-up for all metal sulfide syntheses. The glassware includes: (I) three neck round bottom flask housing the metal precursor and any additional oleates, (II) thermocouple (pictured as thermometer here) for tracking the temperature of the reaction, (III) additional funnel used for the hot addition of thiourea to the metal precursor, (IV) condenser and gas adapter used to add an inert gas (N_2 or Ar) to the reaction vessel.

6.4 Experimental Set-Up for NMR Scale Syntheses

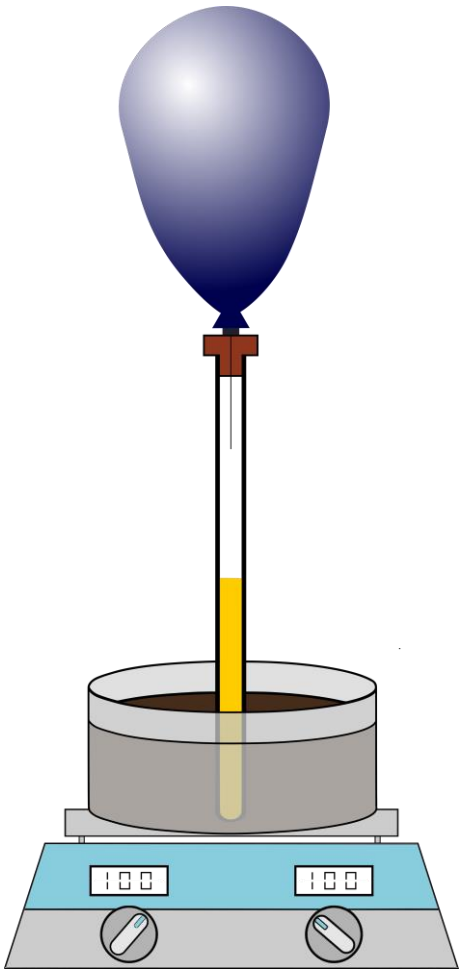

Figure S17. Experimental set-up for NMR scale copper and nickel sulfide syntheses. All reagents were packed inside the glovebox (no solvent) into the NMR tube. A balloon filled with N_2 was then added to the NMR tube to keep atmosphere inert. The NMR tube was then added to the oil bath for temperature and time studies.

6.4 Gas FTIR Cell Set-Up and Positioning of Gas Ports

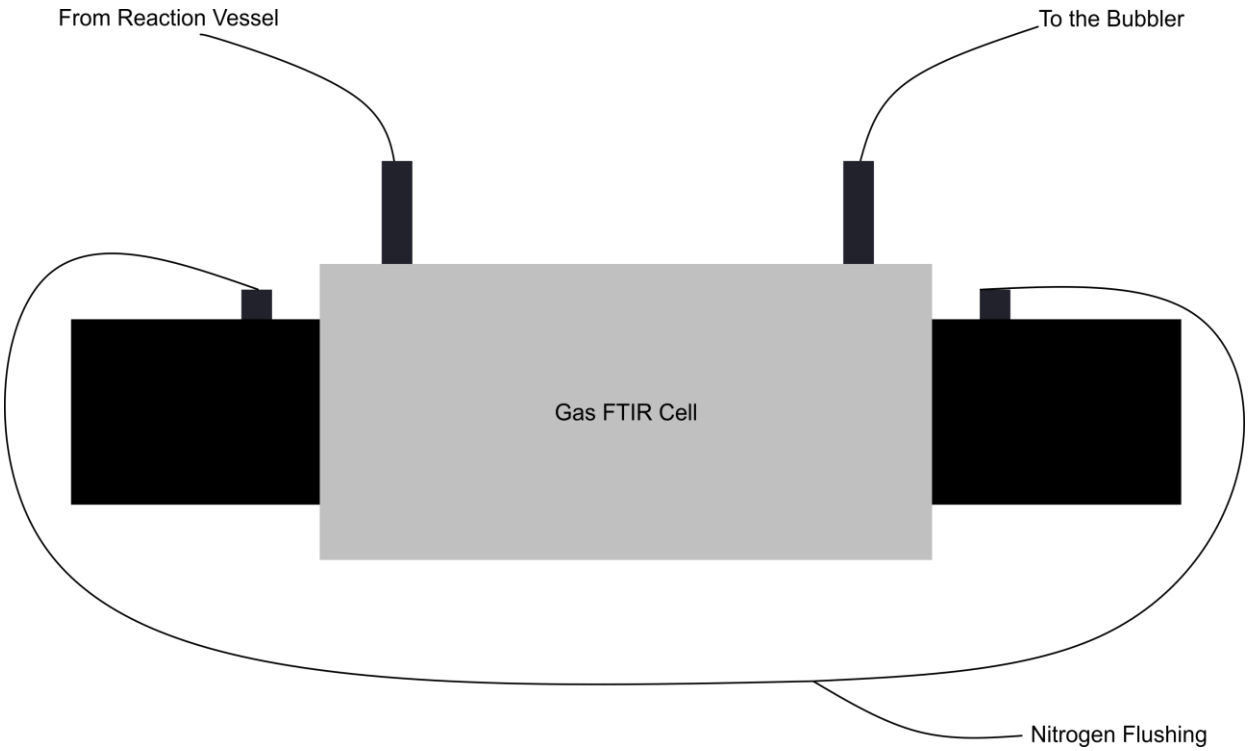

Figure S18. Experimental set-up for gas FTIR experiments. The gas IR cell was positioned inside the spectrometer. Two external ports (outermost gas adapters) were flushed with N_2 for the entire duration of the experiment. The two inner ports were responsible for passing the gas evolved during the reaction. Any gas travelled to the left port and existed through the right port into a bubbler.

7. References

1. Rao, M. H., Pallepogu, R. & Muralidharan, K. Unexpected formation of ammonium thiocyanate from the reaction of aqueous hydroxylamine with carbon disulfide. *Inorg Chem Commun* **13**, 622–624 (2010).

2. Grønvold, F. & Westrum, E. F. Heat capacities of iron disulfides Thermodynamics of marcasite from 5 to 700 K, pyrite from 300 to 780 K, and the transformation of marcasite to pyrite. *J Chem Thermodyn* **8**, 1039–1048 (1976).

3. Erd, R. C., Evans Jr., H. T. & Richter, D. H. Smythite, A New Iron Sulfide, and Associated Pyrrhotite from Indiana*. *American Mineralogist* **42**, 309–333 (1957).

4. Subramani, T., Lilova, K., Abramchuk, M., Leinenweber, K. D. & Navrotsky, A. Greigite (Fe3S4) is thermodynamically stable: Implications for its terrestrial and planetary occurrence. *Proc Natl Acad Sci U S A* **117**, 28645–28648 (2020).

5. Waldner, P. & Sitte, W. Digenite Cu 2-xS: Thermodynamic analysis of sulfur activities. *Monatsh Chem* **143**, 1215–1218 (2012).

6. Waldner, P. Solid-State Phase Equilibria of the Cu-S System: Thermodynamic Modeling. *J Phase Equilibria Diffus* **39**, 810–819 (2018).

7. Cemic, L. & Kleppa, O. J. High temperature calorimetry of sulfide systems. I. Thermochemistry of liquid and solid phases of Ni + S. *Geochim Cosmochim Acta* **50**, 1633–1641 (1986).

8. Cemič, L. & Kleppa, O. J. High temperature calorimetry of sulfide systems - III. Standard enthalpies of formation of phases in the systems Fe-Cu-S and Co-S. *Phys Chem Miner* **16**, 172–179 (1988).

9. Rosenquist, T. A Thermodynamic Study of Iron, Cobalt, and Nickel Sulfides. *Journal of the Iron and Steel Institute* **176**, 37–57 (1954).